Quadratic induced polarization by an external heavy charge in an electron gas

A. Bergara,* I. Campillo, and J. M. Pitarke
Materia Kondentsatuaren Fisika Saila, Zientzi Falkultatea, Euskal Herriko Unibertsitatea, 644 Posta kutxatila, 48080 Bilbo, Basque Country, Spain

P. M. Echenique
Materialen Fisika Saila, Kimika Falkultatea, Euskal Herriko Unibertsitatea, 1072 Posta kutxatila, 20080 Donostia, Basque Country, Spain

(Received 6 May 1997; revised manuscript received 30 June 1997)

We have studied the many-body nonlinear interactions between a heavy ion and a solid, modeled by jellium. Once the retarded prescription for the quadratic response function of the medium is obtained, a derivation of the second-order nonlinear induced polarization charge, proportional to $(Z_1)^2$ (Z_1 being the ion charge), and the potential that it originates are presented. These magnitudes are evaluated numerically using the full random-phase approximation to describe the shielded interaction. A comparison with the linear contribution allows us to discuss the validity of the perturbative approach. [S0163-1829(97)07447-X]

I. INTRODUCTION

A swift charged particle penetrating a solid causes an oscillating distortion in the electronic density of the medium. Pioneering work on dynamic screening was performed by Neufeld and Ritchie.[1] They were the first to present the evaluation of the induced potential and the density wake by using a local dielectric function as the linear response of the medium. Since this work much research has been oriented to the study of these quantities.[2–5] In the late seventies, Echenique, Ritchie, and Brandt[4] studied the spatial distribution of the wake within the plasmon-pole approximation to the dielectric function. Then, Mazarro, Echenique, and Ritchie[5] calculated the wake potential and density fluctuations in the full random-phase approximation (RPA), also on the basis of a linear response of the medium. All these previous studies are based upon a linear response of the target. This happens to be a good approximation when the velocity of the projectile is much greater than the average velocity of target electrons (typically v_F, the Fermi velocity); however, in the case of projectiles moving with smaller velocities, nonlinearities play an important role for metallic densities ($2<r_s<6$). There exists a variety of experimental conditions where there is a need for a nonlinear theory of the electronic polarization and wake potential. Experimental evidence of the importance of nonlinear effects was first presented by Barkas and co-workers.[6] They measured the different ranges in the stopping power suffered by positive and negative pions, which linear theories predicted to be the same.

The Coulomb explosion of OH^+ ions in carbon foils[7] also indicates that the linear wake potential is not enough to explain the experimental data, higher-order contributions to the induced potential being important. An approximate theory of the nonlinear wake was developed by Faibis and co-workers[7] by using Coulomb scattering, but a nonlinear theory that accounted for collective phenomena was presented by Esbensen and Sigmund[8] in the static electron gas approximation. Nonlinear hydrodynamical descriptions of the wake potential have been formulated recently. Arnau and Zaremba,[9] by introducing a phenomenological friction parameter, obtained results in the low-velocity regime. Dorado, Crawford, and Flores[10] have used the hydrodynamical model to perform a perturbative expansion in the electronic density up to the first nonlinear term with respect to the charge of the probe in its high-velocity regime. It has been also shown[11] that the second-order wake coincides, within a nonlinear quantum hydrodynamical model, with plasmon-pole-like approximations to the corresponding full RPA scheme.

The analytical study of the quadratic response function of an electron gas has enabled to calculate, within the RPA, the magnitude of various nonlinear effects such as the first nonlinear contribution to the energy loss of a charged particle,[12–15] double plasmon excitation probabilities,[16] and, in particular, the second-order electronic wake.[17,18] Analytical evaluations of the triple vertex fermion loop were done by Cenni and Saracco[19] and Richardson and Ashcroft.[20] Explicit expressions for the imaginary part of this loop have been given in Refs. 14 and 15, in terms of a sum of particle and hole states. Recently, Rommel and Kalman[21] have studied the conservation sum rules and the frequency moments of the quadratic density response function.

In this paper we present a diagrammatic approach to evaluate the second-order induced potential and polarizability charge distribution when a charged particle penetrates a homogeneous electron gas. Our calculations are valid for nonrelativistic arbitrary velocities, and are performed in the full RPA. Section II is devoted to the quantum theory of the induced potential. In Sec. III we derive the quadratic induced potential and we also define the retarded second-order response function. In Sec. IV numerical results for the spatial distribution of the quadratic induced polarization charge and potential for different velocities and electron densities are presented; comparison with the linear wake and previous approaches is done and the validity of the perturbative treatment is discussed. The most relevant conclusions of this work are presented in Sec. V. Finally, an Appendix with the prescription to pass from the time-ordered to the retarded quadratic response function is added.

II. QUANTUM THEORY OF THE INDUCED POTENTIAL

We consider a point charge $Z_1 e$ moving with constant velocity v through an isotropic homogeneous electron gas embedded in a uniformly distributed positive background, the so-called *jellium* model. The electric potential operator, at point $\mathbf{r}$, induced by the electron gas, which is disturbed due to the interaction with the external charge, and the positive background is (we use atomic units throughout, i.e, $e^2=\hbar=m_e=1$)

$$V(\mathbf{r})=-\sum_{\mathbf{r}_e}\frac{1}{|\mathbf{r}-\mathbf{r}_e|}+V_{\mathrm{BG}}, \tag{2.1}$$

where $\mathbf{r}_e$ represents the electron position operator, and V_{BG}, the interaction between a test positive unit charge at $\mathbf{r}$ and the positive background. In the representation of second quantization the induced potential reads

$$V(\mathbf{r})=-\Omega^{-1}\sum_{\mathbf{k},\mathbf{q},\lambda}{}' v_{\mathbf{q}} e^{-i\mathbf{q}\cdot\mathbf{r}} a^{\dagger}_{\lambda,\mathbf{k}+\mathbf{q}} a_{\lambda,\mathbf{k}}, \tag{2.2}$$

where $a^{\dagger}_{\lambda,\mathbf{k}}$ and $a_{\lambda,\mathbf{k}}$ are the creation and annihilation operators for electrons, respectively, of well-defined momentum $\mathbf{k}$ and spin state λ, Ω is the normalization volume and $v_{\mathbf{q}}$ is the Fourier transform of the electron-electron bare Coulomb interaction,

$$v_{\mathbf{q}}=\frac{4\pi}{\mathbf{q}^2}. \tag{2.3}$$

The comma on the summation indicates that the term with $\mathbf{q}=0$ is not considered, since it is canceled with the contribution from the positive uniform background. In the following equations the sum over electron spin states will be implicitly considered.

The induced potential, also known as the wake potential, is found as the mean value of the electric potential of Eq. (2.1):

$$\phi(\mathbf{r},t)=\frac{\langle\Phi_0|V^H(\mathbf{r},t)|\Phi_0\rangle}{\langle\Phi_0|\Phi_0\rangle}, \tag{2.4}$$

$V^H(\mathbf{r},t)$ being the electric potential in the Heisenberg representation, and $|\Phi_0\rangle$, the Heisenberg ground state of the total interacting system.

We consider that the external charged particle has a mass much greater than the electronic one, so that recoil effects in the collisions will be neglected and the incoming ion will be treated as an external source of energy and momentum. Therefore, the Hamiltonian of this system has a term related to the electron gas and a second one that describes the interaction between the ion and the electron gas. In the representation of second quantization this Hamiltonian reads

$$H=H_e+H_{i-e}. \tag{2.5}$$

H_e represents the interacting electron gas Hamiltonian:

$$H_e=H_0+H_{e-e}, \tag{2.6}$$

where H_0 is the free electron gas Hamiltonian,

$$H_0=\sum_{\mathbf{k}}\omega_{\mathbf{k}} a^{\dagger}_{\mathbf{k}} a_{\mathbf{k}}, \tag{2.7}$$

with $\omega_{\mathbf{k}}=\mathbf{k}^2/2$, and

$$H_{e-e}=\frac{1}{2\Omega}\sum_{\mathbf{p},\mathbf{p}_1,\mathbf{q}}{}' v_{\mathbf{q}} a^{\dagger}_{\mathbf{p}-\mathbf{q}} a_{\mathbf{p}} a^{\dagger}_{\mathbf{p}_1+\mathbf{q}} a_{\mathbf{p}_1} \tag{2.8}$$

gives the electron-electron interaction. H_{i-e} represents the interaction between the heavy ion and the electron gas:

$$H_{i-e}=-\frac{Z_1}{\Omega}\sum_{\mathbf{k},\mathbf{q}}{}' v_{\mathbf{q}} e^{-i\mathbf{q}\cdot\mathbf{v}t} a_{\mathbf{k}} a^{\dagger}_{\mathbf{k}+\mathbf{q}}. \tag{2.9}$$

Our system is irreversible due to the explicit time dependence in the interaction with the external charge.

Treating the interaction between the ion and the electron gas separately from the interactions between the electrons in the metal, the above picture allows us to rewrite Eq. (2.4) in the following way:

$$\phi(\mathbf{r},t)=\frac{\langle\Psi_0|U^{\dagger}(t,-\infty)V^I(\mathbf{r},t)U(t,-\infty)|\Psi_0\rangle}{\langle\Psi_0|U^{\dagger}(t,-\infty)U(t,-\infty)|\Psi_0\rangle}, \tag{2.10}$$

where $|\Psi_0\rangle$ represents the ground state of the interacting electron Hamiltonian of Eq. (2.6) and $U(t_1,t_0)$ is the evolution operator.[22] The I superscript indicates that the operators are considered in the Interaction representation where the total electronic Hamiltonian of Eq. (2.6) is included in the ground state and in the time evolution of the operators, and the perturbation comes from the interaction with the external ion. To evaluate the induced potential, the electron-electron interaction and the interaction with the external charge can be studied separately when this representation is considered. In this way, the screening of the induced electronic density may be studied up to infinite order in the electron-electron interaction on the basis of quantum field theory in order to get the self-consistency. Finally, by expanding the evolution operator U up to second order in the external charge (Z_1), the quadratic correction to the wake potential can be obtained, after some rearrangement:

$$\begin{aligned}\phi(\mathbf{r},t)=&\frac{\langle\Psi_0|V^I(\mathbf{r},t)|\Psi_0\rangle}{\langle\Psi_0|\Psi_0\rangle}+i\int_{-\infty}^{\infty}dt_1\Theta(t-t_1)\\&\times\frac{\langle\Psi_0|[H^I_{i-e}(t_1),V^I(\mathbf{r},t)]|\Psi_0\rangle}{\langle\Psi_0|\Psi_0\rangle}\\&-\int_{-\infty}^{\infty}\int_{-\infty}^{\infty}dt_1dt_2\Theta(t-t_1)\Theta(t_1-t_2)\\&\times\frac{\langle\Psi_0|[[V^I(\mathbf{r},t),H^I_{i-e}(t_1)],H^I_{i-e}(t_2)]|\Psi_0\rangle}{\langle\Psi_0|\Psi_0\rangle},\end{aligned} \tag{2.11}$$

where $[a,b]=ab-ba$. The first term does not contribute, since it corresponds to the induced potential without any external perturbation. The second and third terms represent the linear and quadratic contributions to the induced potential, respectively.

A. The linear induced potential

After the introduction of Eqs. (2.2) and (2.9) into Eq. (2.11), the induced potential is up to the first order in the ion charge:

$$\phi_1(\mathbf{r},t)=\frac{Z_1}{\Omega^2}\int_{-\infty}^{\infty}dt_1\sum_{\mathbf{q},\mathbf{q}_1} v_{\mathbf{q}}v_{\mathbf{q}_1}e^{i\mathbf{q}\cdot\mathbf{r}}e^{i\mathbf{q}_1\cdot\mathbf{v}t_1}\chi^R_{\mathbf{q}}(t,t_1), \tag{2.12}$$

where

$$\chi^R_{\mathbf{q}}(t,t_1)=-i\Theta(t-t_1)\frac{\langle\Psi_0|[n^I_{\mathbf{q}}(t),n^I_{\mathbf{q}}(t_1)]|\Psi_0\rangle}{\langle\Psi_0|\Psi_0\rangle} \tag{2.13}$$

is the retarded density-density correlation function, and

$$n^I_{\mathbf{q}}(t)=\Omega^{-1}\sum_{\mathbf{k}}[a^I_{\mathbf{k}}(t)]^{\dagger}a^I_{\mathbf{k}+\mathbf{q}}(t), \tag{2.14}$$

is the Fourier transform of the number density fluctuation operator. The exact linear density response function of the medium is represented through the above-defined density-density retarded correlation function. The causality of the response function is preserved due to the retarded way in which it is defined. Furthermore, it is interesting to analyze the relation that exists between the time-ordered response function,

$$\chi^{\mathrm{TO}}_{\mathbf{q}}(t,t_1)=-i\frac{\langle\Psi_0|T[n^I_{\mathbf{q}}(t)n^I_{\mathbf{q}}(t_1)]|\Psi_0\rangle}{\langle\Psi_0|\Psi_0\rangle}, \tag{2.15}$$

and the retarded one. After making the time Fourier transformation on both functions, the Lehmann representation[23] can be used to conclude that the retarded response function may be obtained from the time-ordered one once all the imaginary parts of the frequencies are turned to be positive.

The Gell-Mann and Low and Wick theorems may be used in order to evaluate the linear time-ordered response, and the defined prescription allows us to obtain the retarded one in a straight way. The Fourier transform of the density-density correlation function of Eq. (2.15), χ_q [here q represents the tetramomentum $(\mathbf{q},\omega)$], can be represented diagrammatically by a full two-point vertex or bubble. In the RPA it is approximated by summing over the infinite set of diagrams containing a string of empty bubbles.[24]

We already know the prescription to go from the time-ordered response function to the retarded one. Thus, after extending to the continuum phase space on the momentum variable, the result we obtain for the induced potential is

$$\phi_1(\mathbf{r},t)=Z_1\int\frac{d^3\mathbf{q}}{(2\pi)^3}e^{i(\mathbf{q}\cdot\mathbf{r}-\omega t)}v_{\mathbf{q}}[(\epsilon^R_{\mathbf{q},\omega})^{-1}-1], \tag{2.16}$$

where $\omega=\mathbf{q}\cdot\mathbf{v}$ and ϵ^R_q represents the retarded dielectric function of the medium, in the RPA:

$$\epsilon^R_q=1-v_{\mathbf{q}}(\chi^0_q)^R, \tag{2.17}$$

$(\chi^0_q)^R$ representing the so-called retarded linear density response function of the noninteracting electron gas.[24]

Equation (2.16) exactly coincides with the standard expression for the linear induced potential.[25]

For high velocities of the ion, the zero-point motion of the electron gas can be neglected and it can be considered, therefore, as if it were at rest. Thus, in this approximation all momenta of the electrons are set equal to zero and Eq. (2.17) leads to the well-known static electron gas approximation for the dielectric function:

$$\epsilon^R_q=1-\frac{\omega_p^2}{(\omega+i\eta)^2-(\alpha^{sg}_{\mathbf{q}})^2}, \tag{2.18}$$

where $\alpha^{sg}_{\mathbf{q}}=\mathbf{q}^2/2$, η is an infinitesimal positive quantity and $\omega_p=\sqrt{4\pi n_0}$ represents the plasma frequency for the electron gas.

Finally, the velocity distribution of the electron gas, which is completely neglected in the static electron gas approximation, can be accounted for approximately by introducing the plasmon-pole approximation to the response function, which is the same as Eq. (2.18) but with

$$\alpha^{pp}_{\mathbf{q}}=\sqrt{\beta^2\mathbf{q}^2+\mathbf{q}^4/4}, \tag{2.19}$$

where

$$\beta^2=\frac{3}{5}\mathbf{q}_F^2 \tag{2.20}$$

represents the mean-square velocity of the electron gas and q_F is the Fermi momentum defined by the equilibrium host electronic density n_0 as $(3\pi^2n_0)^{1/3}$. This approximation can also be obtained from a hydrodynamic model if the von Weiszacker term is included to account for the individual electron behavior.

III. THE QUADRATIC INDUCED POTENTIAL

In the present section we will analyze the term that is proportional to the second power of the ion charge in the expression of the induced potential of Eq. (2.11):

$$\phi_2(\mathbf{r},t)=-\int_{-\infty}^{\infty}\int_{-\infty}^{\infty}dt_1dt_2\Theta(t-t_1)\Theta(t_1-t_2)\times\frac{\langle\Psi_0|[[V^I(\mathbf{r},t),H^I_{i-e}(t_1)],H^I_{i-e}(t_2)]|\Psi_0\rangle}{\langle\Psi_0|\Psi_0\rangle}. \tag{3.1}$$

In the representation of second quantization,

$$\phi_2(\mathbf{r},t)=\frac{Z_1^2}{\Omega^2}\int_{-\infty}^{\infty}dt_1dt_2\sum_{\mathbf{q},\mathbf{q}_1,\mathbf{q}_2} v_{\mathbf{q}}v_{\mathbf{q}_1}v_{\mathbf{q}_2}\times e^{i\mathbf{q}\cdot\mathbf{r}}e^{i\mathbf{q}_1\cdot\mathbf{v}t_1}e^{i\mathbf{q}_2\cdot\mathbf{v}t_2}Y^R_{\mathbf{q},\mathbf{q}_1,\mathbf{q}_2}(t,t_1,t_2), \tag{3.2}$$

which is written in terms of the retarded quadratic response function of the medium:

$$Y^R_{\mathbf{q},\mathbf{q}_1,\mathbf{q}_2}(t,t_1,t_2) = \Theta(t-t_1)\Theta(t_1-t_2) \times \frac{\langle\Psi_0|[[n^I_{\mathbf{q}}(t),n^I_{\mathbf{q}_1}(t_1)],n^I_{\mathbf{q}_2}(t_2)]|\Psi_0\rangle}{\langle\Psi_0|\Psi_0\rangle}. \tag{3.3}$$

This function contains the product of three electronic density operators. The quantum field theory for systems in equilibrium cannot be applied in order to evaluate the defined retarded quadratic response function in a direct way; one should use, instead, the Keldysh[26] formalism, which is adequate for irreversible processes. However, a method similar to the one considered in the previous section may be used in the study of the relationship between the retarded quadratic response function and the following time-ordered one:

$$Y^{\mathrm{TO}}_{\mathbf{q},\mathbf{q}_1,\mathbf{q}_2}(t,t_1,t_2) = \frac{1}{2}\frac{\langle\Psi_0|T[n^I_{\mathbf{q}}(t)n^I_{\mathbf{q}_1}(t_1)n^I_{\mathbf{q}_2}(t_2)]|\Psi_0\rangle}{\langle\Psi_0|\Psi_0\rangle}. \tag{3.4}$$

After using the Lehmann representation (see the Appendix), defining the frequencies ω, ω_1, and ω_2 as the Fourier transform variables of t, t_1, and t_2, respectively, and performing the integrations over the time variables of Eq. (3.2), we find

$$\phi_2(\mathbf{r},t) = Z_1^2\int \frac{d\mathbf{q}}{(2\pi)^3}\frac{d\mathbf{q}_1}{(2\pi)^3}e^{i\mathbf{q}\cdot(\mathbf{r}-\mathbf{v}t)}v_{\mathbf{q}}v_{\mathbf{q}_1}v_{\mathbf{q}+\mathbf{q}_1}Y^R_{\mathbf{q},\mathbf{q}_1,\mathbf{q}+\mathbf{q}_1} \times(\omega,\omega_1,-\omega-\omega_1), \tag{3.5}$$

where $\omega=\mathbf{q}\cdot\mathbf{v}$ and $\omega_1=\mathbf{q}_1\cdot\mathbf{v}$. As demonstrated in the Appendix, when these frequencies are turned into $\omega+i\eta$, $\omega_1-i\eta$, and $\omega_2-i\eta$ in the time-ordered quadratic response function we get the retarded one. A change in the $\mathbf{q}_1$ wavevector sign makes all the frequency imaginary parts positive in the retarded function, resulting, therefore, in the usual retarded prescription.

Thus, as we did in the evaluation of the linear induced potential, we can apply the defined prescription to derive the second order Y^R after the evaluation of the corresponding time-ordered response function. In the RPA, the triple vertex is approximated by three legs with an infinite sum of empty bubbles, already defined in the previous section, and one fermion empty triple vertex loop:[17]

$$M_{q,q_1} = -2i\int\frac{d^4k}{(2\pi)^4}G^0_kG^0_{k+q}G^0_{k+q_1}, \tag{3.6}$$

G^0_q being the free particle propagator.

The three point functions M_{q,q_1} and $M_{q,q-q_1}$, represented diagrammatically by empty triangle diagrams with their lines running in opposite directions, give the same contribution, and we define the symmetrized function:

$$M^s_{q,q_1} = \frac{1}{2}\{M_{q,q_1}+M_{q,q-q_1}\}. \tag{3.7}$$

Once we take into account all the previous considerations, the expression we have for the quadratic response function is

$$Y^R_{\mathbf{q},-\mathbf{q}_1,\mathbf{q}-\mathbf{q}_1}(\omega,-\omega_1,-\omega+\omega_1) = (\epsilon^R_{\mathbf{q},\omega})^{-1}(\epsilon^R_{\mathbf{q}_1,\omega_1})^{-1}(\epsilon^R_{\mathbf{q}-\mathbf{q}_1,\omega-\omega_1})^{-1}(M^R_{\mathbf{q},\omega;\mathbf{q}_1,\omega_1})^s. \tag{3.8}$$

The expression for the induced potential up to second order in the ion charge is

$$\phi_2(\mathbf{r},t) = Z_1^2\int\frac{d^3\mathbf{q}}{(2\pi)^3}e^{i(\mathbf{q}\cdot\mathbf{r}-\omega t)}v_{\mathbf{q}}\int\frac{d^3\mathbf{q}_1}{(2\pi)^3} \times v_{\mathbf{q}_1}v_{\mathbf{q}-\mathbf{q}_1}(\epsilon^R_{\mathbf{q},\omega})^{-1}(\epsilon^R_{\mathbf{q}_1,\omega_1})^{-1} \times(\epsilon^R_{\mathbf{q}-\mathbf{q}_1,\omega-\omega_1})^{-1}(M^R_{\mathbf{q},\omega;\mathbf{q}_1,\omega_1})^s. \tag{3.9}$$

Once we have obtained the potential induced by the heavy ion, the evaluation of the quadratic polarization induced charge is direct, after using the Poisson equation:

$$\delta n_2(\mathbf{r},t) = -Z_1^2\int\frac{d^3\mathbf{q}}{(2\pi)^3}e^{i(\mathbf{q}\cdot\mathbf{r}-\omega t)}\int\frac{d^3\mathbf{q}_1}{(2\pi)^3} \times v_{\mathbf{q}_1}v_{\mathbf{q}-\mathbf{q}_1}(\epsilon^R_{\mathbf{q},\omega})^{-1}(\epsilon^R_{\mathbf{q}_1,\omega_1})^{-1} \times(\epsilon^R_{\mathbf{q}-\mathbf{q}_1,\omega-\omega_1})^{-1}(M^R_{\mathbf{q},\omega;\mathbf{q}_1,\omega_1})^s. \tag{3.10}$$

The most important nonlinear contribution corresponds to the spatial range close to the ion. Therefore, the derivative of the potential will change in an important way when it is evaluated at the position of the charged particle. The energy that the ion loses when it excites the medium can be evaluated through the induced electric field, $\mathbf{E}=-\boldsymbol{\nabla}\phi$, at the position of the ion, and one obtains from Eqs. (2.16) and (3.9) the same contributions for the stopping as derived in Refs. 14 and 15.

For high velocities, one can set all $\mathbf{k}$ equal to zero in Eq. (3.6) to obtain the static electron gas approximation for $(M^R_{q,q_1})^s$:

$$\begin{aligned}(M^R_{q,q_1})^s = -n_0\{&\omega_1(\omega-\omega_1)\omega^2_{\mathbf{q}}-\omega(\omega-\omega_1)\\ &\times\omega^2_{\mathbf{q}_1}-\omega\omega_1\omega^2_{\mathbf{q}-\mathbf{q}_1}+(\omega-\omega_1)\omega_{\mathbf{q}}\omega_{\mathbf{q}_1}\\ &+\omega_1^2\omega_{\mathbf{q}}\omega_{\mathbf{q}-\mathbf{q}_1}+\omega^2\omega_{\mathbf{q}_1}\omega_{\mathbf{q}-\mathbf{q}_1}-\omega_{\mathbf{q}}\omega_{\mathbf{q}_1}\omega_{\mathbf{q}-\mathbf{q}_1}\\ &\times(\omega_{\mathbf{q}}+\omega_{\mathbf{q}_1}+\omega_{\mathbf{q}-\mathbf{q}_1})\}\{[(\omega+i\eta)^2-(\alpha^{sg}_{\mathbf{q}})^2]\\ &\times[(\omega_1+i\eta)^2-(\alpha^{sg}_{\mathbf{q}_1})^2]\\ &\times[(\omega-\omega_1+i\eta)^2-(\alpha^{sg}_{\mathbf{q}-\mathbf{q}_1})^2]\}^{-1},\end{aligned} \tag{3.11}$$

with $\omega_{\mathbf{q}}=\mathbf{q}^2/2$. In the plasmon-pole approximation $\alpha^{sg}_{\mathbf{q}}$ must be replaced in Eq. (3.11) by $\alpha^{pp}_{\mathbf{q}}$.[18]

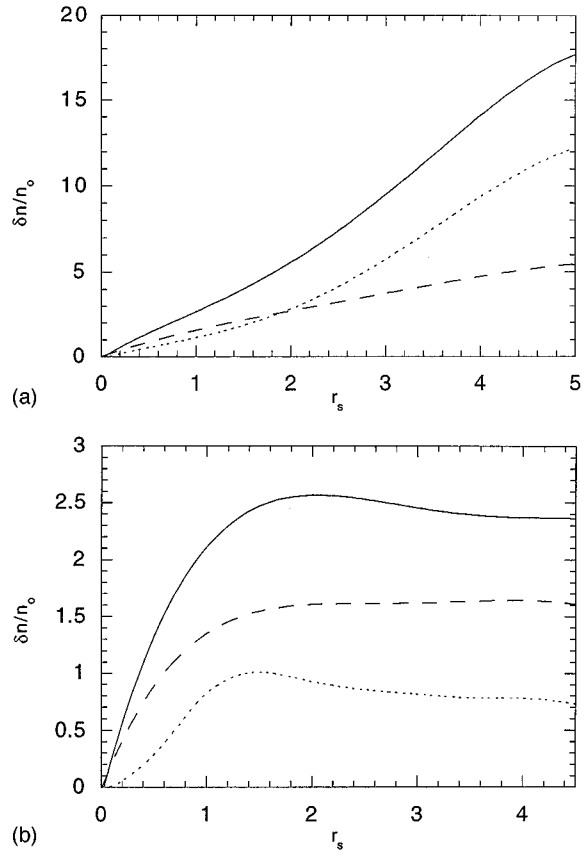

FIG. 1. First- (dashed line) and second- (dotted line) order induced density, as derived from the RPA, at the position of the ion of charge unity ($Z_1=1$) moving with velocities (a) $v=0.5$ and (b) $v=2$, as a function of r_s. The total induced density, up to second order in the ion charge, is represented by a solid line. Nonlinear effects are less important as the velocity of the ion and/or the electronic density of the medium increase.

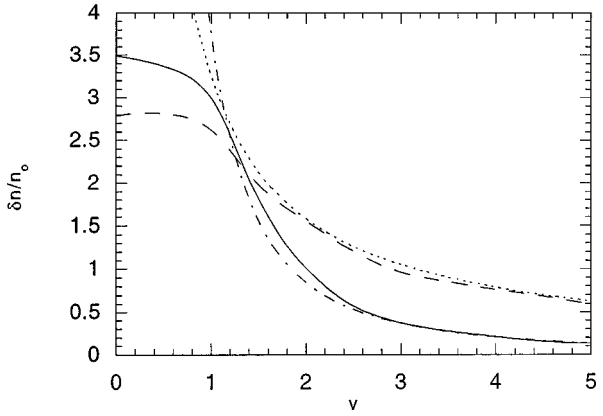

FIG. 2. First (dashed line) and second (solid line) -order induced density, as derived from the RPA, at the position of an ion of charge unity moving in a medium of $r_s=2.07$, as a function of the velocity of the ion. First- and second-order scattering theory results (Ref. 25) are represented by dotted and dashed-dotted lines. When the velocity of the ion is higher than v_F the scattering theory results coincide with the RPA.

IV. RESULTS

In this section, results for the quadratic induced polarization density and potential are presented, as obtained in the full RPA.

The first-order induced density at the position of low-velocity ions gives $\delta n_1 > n_0$, as will be shown. This indicates that the linear theory is not enough to obtain this magnitude. On the other hand, the induced electronic density decreases very fast as the velocity of the ion is increased, where the linear approximation becomes valid. The analysis of the nonlinear terms has to be made with regard to magnitudes characterizing our interacting system: v, the velocity of the incoming charged particle, and $r_s(r_s=(3/4n_0\pi)^{1/3})$, the electron density parameter. Also, the perturbation becomes larger as the ion charge is increased; nevertheless, in the following discussion a projectile of unit charge will be considered.

In Figs. 1(a) and 1(b) first- and second-order contributions to the induced electron density at the position of the ion are presented, as a function of r_s, for projectile velocities of 0.5 and 2 times the Bohr velocity. It is obvious from these figures that nonlinear corrections are smaller for higher electron densities of the medium (lower r_s), which is due to the well-known fact that at higher densities the kinetic energy of the electron gas increases and the potential energy of the ion becomes, therefore, a relatively smaller perturbation.[18–26] This can be seen in Fig. 1(a), where the second-order contribution gains the linear one at a certain r_s value. On the other hand, nonlinear effects are less important as the ion velocity increases, so that the quadratic contribution is always lower than the linear one for $v=2$, as shown in Fig. 1(b). In the high-velocity limit of the incoming ion ($v \gg v_F$), it corresponds to the high r_s range in Fig. 1(b); the relative induced density at the position of the ion is constant with respect to the density of the medium as shown in this figure and will be explained later.

In Fig. 2 we present the evaluation of the linear and quadratic induced densities at the position of the charged particle, as it passes through a medium with a density parameter equal to that of aluminum, $r_s=2.07$, as a function of the velocity of the ion. It is easy to see that when the velocity of the incoming ion is lower than the characteristic velocity of the electrons in the metal v_F, the induced density remains almost constant. This velocity range corresponds to a highly nonlinear regime, where the quadratic contribution is larger than the linear one. This indicates the breakdown of the perturbation theory in order to evaluate the induced density at the position of the ion. For velocities higher than v_F, the quadratic induced density decreases faster than the linear one and becomes lower for a certain velocity, recovering, therefore, the applicability of the perturbation theory in the high-velocity regime.

With the assumption of independent, individual, elastic electron scattering the induced density at the position of a heavy particle of charge Z_1 is given by the following expression:[27]

$$\frac{\delta n}{n_0}=\frac{2\pi\mu}{1-e^{-2\pi\mu}}, \tag{4.1}$$

with $\mu=Z_1/v$. For high velocities and small ion charges, we can expand this result up to second order in Z_1/v to obtain

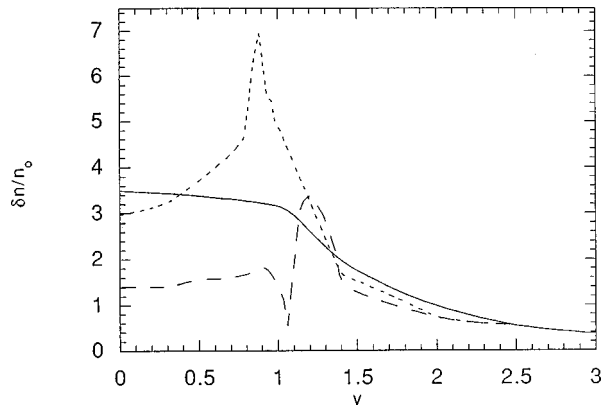

FIG. 3. Second-order induced density at the position of an ion of charge unity moving in a medium of $r_s=2.07$ as a function of the velocity, obtained from different approximations: RPA (full line), plasmon-pole (dashed line), and static electron gas (dotted line). The approximating models give correct results for velocities over 2.5.

$$\frac{\delta n}{n_0}=\frac{\pi Z_1}{v}+\frac{\pi^2 Z_1^2}{3v^2}+O(Z_1/v)^3. \tag{4.2}$$

It can be proved that the first term coincides with the linear contribution obtained in the high-velocity regime.[4] The second term also coincides with the calculated quadratic contribution of Eq. (3.10) when the velocity of the ion is high compared with v_F, as can be seen in Fig. 2. In the high-velocity range there is, therefore, no contribution for this quantity coming from collective excitations, *plasmons*.

The induced electronic density is very strong close to the position of the ion. Thus, the range of validity of the linear perturbation theory decreases when the induced density at the position of the ion is analyzed. For a slow ion, the induced density at its position will be given by the bound state[28] that the positive charged ion can have, but this is not studied here. We would need to go to infinite order[29] in the interaction with the external ion in order to get this result.

It is interesting to study the contribution to the induced polarization charge obtained by two different approximations to the RPA: the plasmon-pole and the static electron gas. In both cases we are approximating all the excitations of the system to plasmons with an extended dispersion curve that for large momentum emulates the contribution coming from the particle-hole spectrum in the RPA. Therefore, these models are only meaningful at high velocities of the ion, when plasmon excitation is possible. We have an strong peak just at the plasmon threshold velocity, when the ion has enough energy to excite a real plasmon. In Fig. 3 we can analyze the differences on the magnitudes and positions of the peaks when the mentioned models are considered. The lowest velocity needed to excite a plasmon corresponds to the static electron gas approximation and the higher one to the RPA. As the momentum phase space where the maximum energy transfer line, $\omega=|\mathbf{q}|v$, close to the plasmon dispersion curve is longer in the plasmon-pole approximation, due to the linear term included in its dispersion relation, it is reasonable to think that this model will have the most striking antiscreening effect. On the other hand, the momentum range where

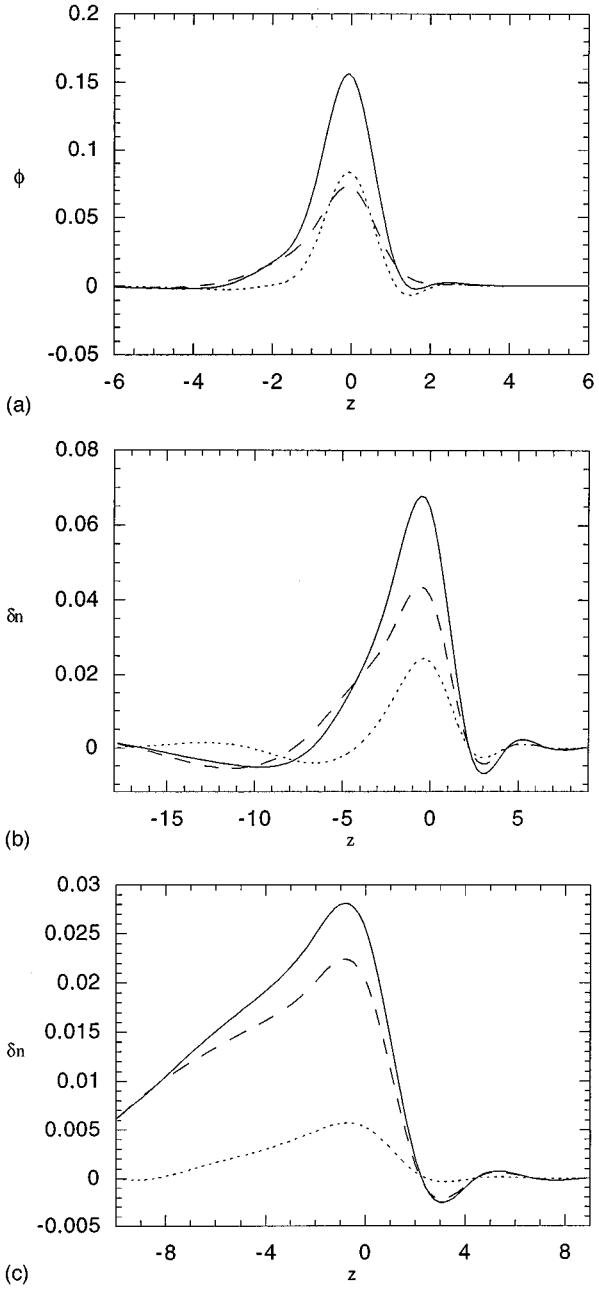

FIG. 4. First- (dashed line) and second- (dotted line) order induced density, as derived in the RPA, along the axis of motion for a particle of charge unity ($Z_1=1$) moving with a velocity (a) $v=0.5$, (b) $v=2$, and (c) $v=4$ in a medium of $r_s=2.07$. The total induced density, up to the second order in the ion charge, is represented by a solid line. At high velocities, oscillations in front and behind the ion are obvious.

the plasmon is well defined is, in the RPA, much shorter than in the other models, so that there is not such a peak when a plasmon is excited in this approximation. Nevertheless, these models are not good enough in this velocity range, in which particle-hole excitations should be included in a proper way.

Figures 4(a), 4(b), and 4(c) exhibit the linear and quadratic induced polarization charge, as derived from the RPA, along the trajectory of the projectile in a medium with $r_s=2.07$ and for three velocities of the ion, $v=0.5$, 2, and 4. For a velocity lower than v_F Fig. 4(a) shows that the main

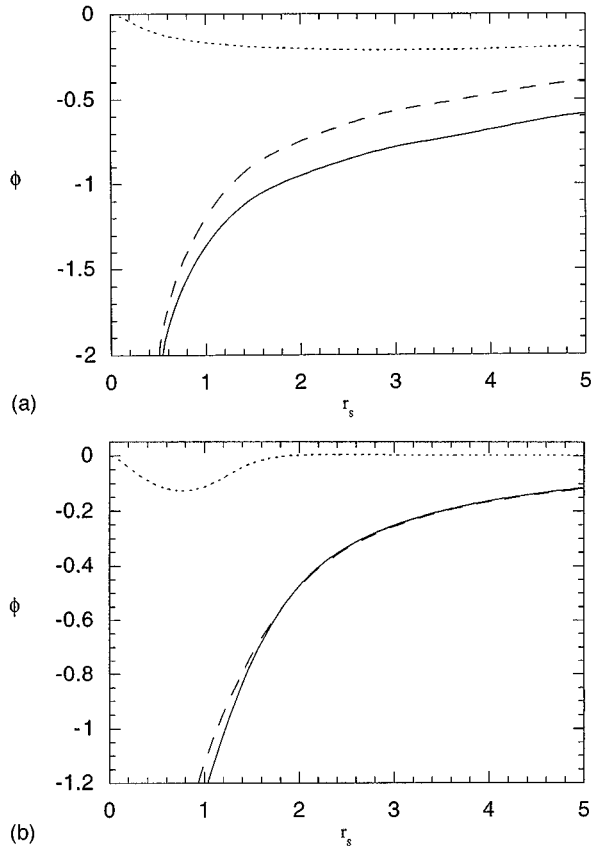

FIG. 5. First- (dashed line) and second- (dotted line) order induced potential, as derived from the RPA, at the position of an ion of charge unity ($Z_1=1$) moving with velocities (a) $v=0.5$ and (b) $v=2$, as a function of r_s. The total induced potential, up to second order in the ion charge, is represented by a solid line. The nonlinear contribution appears to be always lower than the linear one.

induced density is concentrated around the position of the ion, which makes nonlinear effects become very important close to this region. In Figs. 4(b) and 4(c) one sees distinctive oscillations of the induced density in the region behind the particle once the ion has enough energy to excite a plasmon. The wavelength of the oscillation in the linear contribution is $\simeq 2\pi v/\omega_p$.[4] However, when quadratic contributions are analyzed the present wavelength is just half of the previous one, $\simeq \pi v/\omega_p$. Preceding the particle, a bow wave with smaller amplitude appears, both linear and quadratic contributions having the same wavelength, $\simeq 2\pi/v$. This is the de Broglie wavelength of an electron in the medium viewed from the rest frame of the ion and after suffering from a frontal collision with it.

We will do a similar analysis in order to study the induced potential. Figures 5(a) and 5(b) show the first- and the second-order contribution to the wake potential for two velocities of the ion, $v=0.5$ and 2 as a function of the r_s parameter of the medium. It is obvious that quadratic terms are for these velocities always smaller than the linear ones, which is not the case for the induced density. The induced density is a highly nonlinear magnitude at the position of the ion, but as the induced potential is an integrated magnitude of the density over the whole space, it becomes much smoother when the wake potential is evaluated at the same position.

Figure 6 exhibits the linear and quadratic induced potentials at the position of a projectile passing through a medium of $r_s=2.07$ as a function of the velocity of the ion. We can make the same comments as for the induced density in Fig. 2, but it is interesting to remark that perturbation theory is valid to evaluate the induced potential, since the quadratic contribution remains much smaller than the linear one over the whole range of projectile velocities and electron densities of the medium.

Figures 7(a), 7(b), and 7(c) show first- and second-order contributions to the wake potential for three velocities of the ion, one is lower than the plasmon threshold ($v=0.5$) and the other two are higher ($v=2$ and 4). As observed for the induced density, the plasmon threshold velocity determines the separation between two different regimes. When the energy of the projectile is just enough to excite a plasmon, a characteristic oscillation appears trailing the position of the ion, both in the linear and the quadratic contributions, with the same wavelengths than for the induced density in Figs. 4(b) and 4(c). It is interesting to remark that we can observe a high maximum peak for the quadratic induced potential behind the position of the ion in the low velocity range, which is absent in the linear contribution. On the other hand, the quadratic contribution has a bow wave preceding the particle when its velocity is larger than v_F. The origin and the wavelength of this oscillation are the same as those we found in the induced density ($\simeq 2\pi/v$), but not so pronounced. Although these oscillations are also present in the linear wake, they have such a small amplitude that they cannot be observed in the linear case.

Figure 8(a) displays the linear and quadratic wake potential surface as calculated for a projectile moving with velocity $v=2$ in a medium with $r_s=2.07$. Figure 8(b) shows a detail of the quadratic contribution to the wake. It can be seen that it is only significant on the moving axis of the projectile, decaying much faster than the linear contribution out from this axis.

V. CONCLUSIONS

First of all, we have developed a many-body theoretical scheme to derive the retarded quadratic response function of

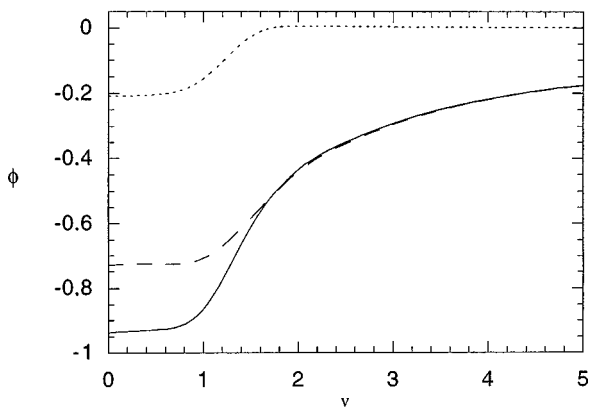

FIG. 6. First- (dashed line) and second- (dotted line) order induced potential, as derived from the RPA, at the position of an ion of charge unity moving in a medium of $r_s=2.07$, as a function of the velocity of the ion. Nonlinear effects decrease as the velocity of the ion increases.

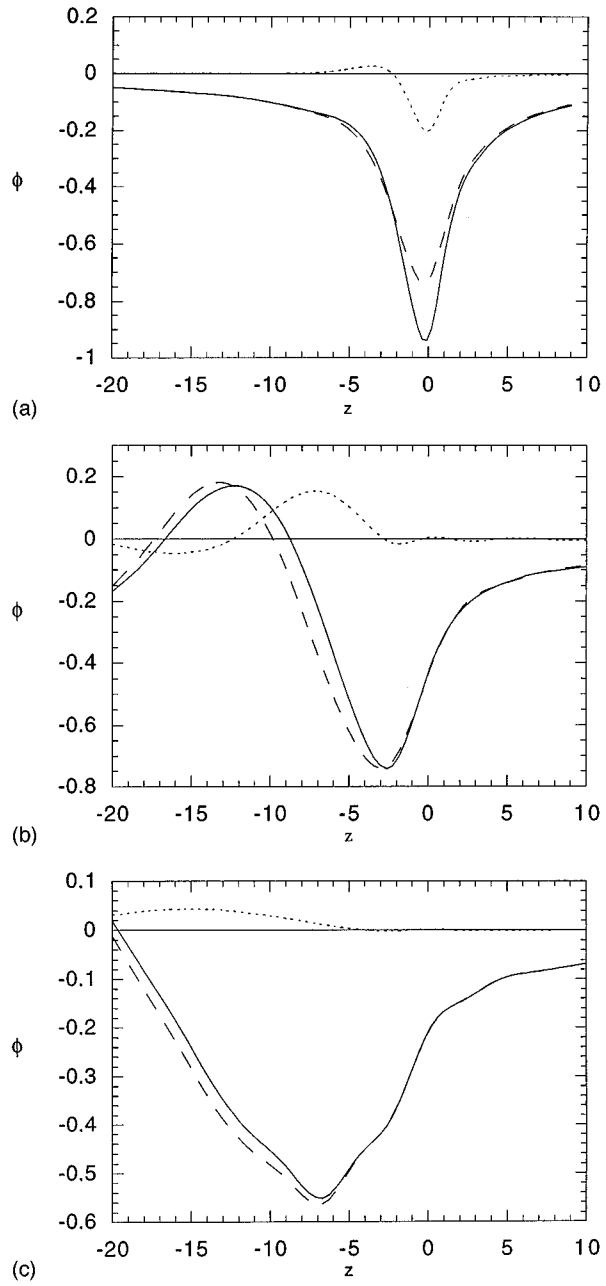

FIG. 7. First- (dashed line) and second- (dotted line) order induced potential in the RPA along the axis of motion for a particle of charge unity ($Z_1=1$) moving with a velocity $v=0.5$ (a), $v=2$ (b), and $v=4$ (c) in a medium of $r_s=2.07$. The total induced potential, up to second order in the ion charge, is represented by a solid line. The nonlinear wake presents the same kind of oscillations as the induced density.

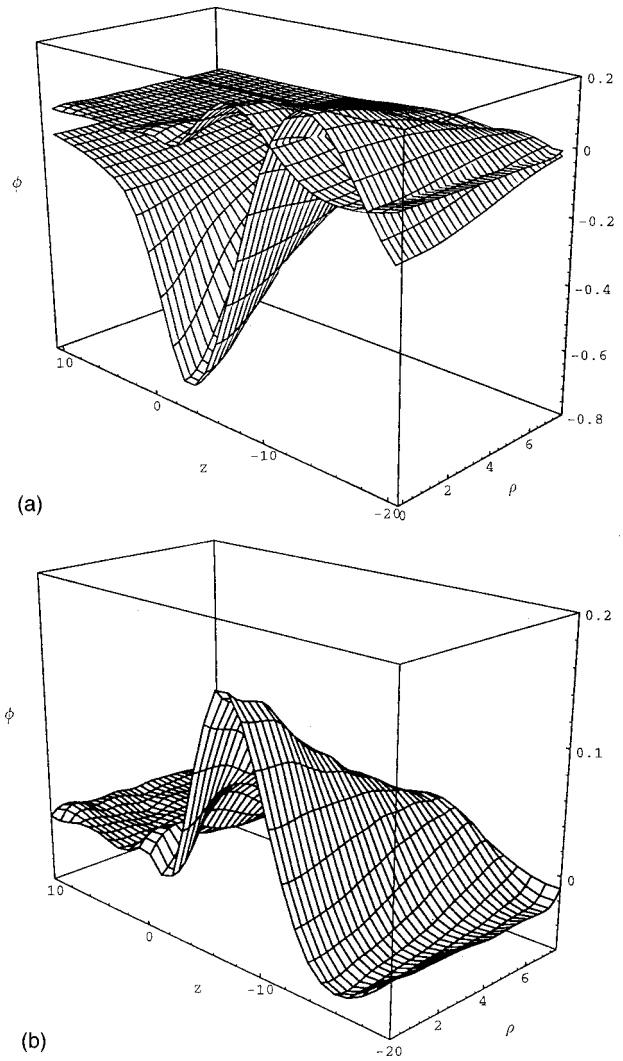

FIG. 8. (a) Linear and second-order surface potential in cylindrical coordinates (ρ,z) with respect to the position of an ion of charge unity moving with $v=2$ in a medium of $r_s=2.07$, as derived in the RPA. (b) A detailed figure of second-order surface potential. It is obvious that the quadratic contribution is significant only on the moving axis of the projectile.

a homogeneous electron gas. This function is the main ingredient to evaluate, for a wide range of nonrelativistic velocities of the incoming particle, the quadratic contribution to the induced density and potential in the full random-phase approximation.

It has been shown that both linear and quadratic contributions to the wake potential exhibit in the region behind the particle oscillations with different wavelengths, $2\pi v/\omega_p$ and $\pi v/\omega_p$; nonlinearities being most important along the axis of motion. At low velocities the wake potential is diminished at the position of the ion, as a consequence of the nonlinearity of the response of the medium, which makes the first minimum deeper, and, on the other hand, the wavelength for the oscillations behind the particle is smaller. At higher velocities the nonlinearity of the wake is negligible. As for the potential, the wavelength of the oscillations in the induced electron density is smaller, as a consequence of the nonlinearity of the response.

ACKNOWLEDGMENTS

We wish to acknowledge the support of the University of the Basque Country and the Basque Unibertsitate eta Ikerketa Saila under Contract Nos. UPV063.310-EA001/95, UPV063.310-EA056/96, GV063.310-0017/95 and Iberdrola SA.

APPENDIX

In this appendix we will study the analytic relation that exists between the time-ordered quadratic response function:

$$Y^{\mathrm{TO}}_{\mathbf{q},\mathbf{q}_1,\mathbf{q}_2}(t,t_1,t_2)=\frac{1}{2}\,\frac{\langle\Psi_0|T[n^I_{\mathbf{q}}(t)n^I_{\mathbf{q}_1}(t_1)n^I_{\mathbf{q}_2}(t_2)]|\Psi_0\rangle}{\langle\Psi_0|\Psi_0\rangle} \tag{A1}$$

and the retarded one:

$$\begin{aligned}Y^{R}_{\mathbf{q},\mathbf{q}_1,\mathbf{q}_2}(t,t_1,t_2)=\frac{1}{2}\Bigg\{&\Theta(t-t_1)\Theta(t_1-t_2)\frac{\langle\Psi_0|[[n^I_{\mathbf{q}}(t),n^I_{\mathbf{q}_1}(t_1)],n^I_{\mathbf{q}_2}(t_2)]|\Psi_0\rangle}{\langle\Psi_0|\Psi_0\rangle}\\&+\Theta(t-t_2)\Theta(t_2-t_1)\frac{\langle\Psi_0|[[n^I_{\mathbf{q}}(t),n^I_{\mathbf{q}_2}(t_2)],n^I_{\mathbf{q}_1}(t_1)]|\Psi_0\rangle}{\langle\Psi_0|\Psi_0\rangle}\Bigg\},\end{aligned} \tag{A2}$$

which appears in the evaluation of the second-order induced potential of Eq. (4.2). The diagrammatic method of the quantum field theory may be considered in order to obtain the time-ordered response function. Then, the relation between both functions can be applied in order to obtain the retarded response function, in which we are interested.

We can observe that the quadratic response function appearing in Eq. (3.2) corresponds to the first term in Eq. (A2). However, the symmetrized expression with respect to $(\mathbf{q}_1,t_1)$ and $(\mathbf{q}_2,t_2)$ will be used, as explicitly indicated in Eq. (A2). Both set of variables are internal in the integral expression for the induced potential. Therefore, we can make the previous operation without any change in the final result. The new split function is more symmetric and it is easier to compare with the symmetrized time-ordered one, which is the main aim of this appendix.

First of all, the Y^{TO} function, which corresponds to the following expanded expression, will be analyzed:

$$\begin{aligned}Y^{\mathrm{TO}}_{\mathbf{q},\mathbf{q}_1,\mathbf{q}_2}(t,t_1,t_2)=\frac{1}{2}\Bigg\{&\Theta(t-t_1)\Theta(t_1-t_2)\frac{\langle\Psi_0|n^I_{\mathbf{q}}(t)n^I_{\mathbf{q}_1}(t_1)n^I_{\mathbf{q}_2}(t_2)|\Psi_0\rangle}{\langle\Psi_0|\Psi_0\rangle}\\&+\Theta(t_1-t)\Theta(t-t_2)\frac{\langle\Psi_0|n^I_{\mathbf{q}_1}(t_1)n^I_{\mathbf{q}}(t)n^I_{\mathbf{q}_2}(t_2)|\Psi_0\rangle}{\langle\Psi_0|\Psi_0\rangle}\\&+\Theta(t_1-t)\Theta(t_2-t)\frac{\langle\Psi_0|n^I_{\mathbf{q}_1}(t_1)n^I_{\mathbf{q}_2}(t_2)n^I_{\mathbf{q}}(t)|\Psi_0\rangle}{\langle\Psi_0|\Psi_0\rangle}+1\Leftrightarrow2\Bigg\},\end{aligned} \tag{A3}$$

where $(1\Leftrightarrow2)$ indicates that we have to include the terms that come from the interchanging of the 1 and 2 subindexes in the momentum and time variables in the first three terms explicitly written in Eq. (A3).

The Fourier transformation on time variables of the previously defined time-ordered quadratic response function may be written in the following way:

$$Y^{\mathrm{TO}}_{\mathbf{q},\mathbf{q}_1,\mathbf{q}_2}(\omega,\omega_1,\omega_2)=\int_{-\infty}^{+\infty}dtdt_1dt_2e^{i\omega t}e^{i\omega_1t_1}e^{i\omega_2t_2}Y^{\mathrm{TO}}_{\mathbf{q},\mathbf{q}_1,\mathbf{q}_2}(t,t_1,t_2). \tag{A4}$$

Step by step, the spectral analysis on the first term of the Fourier transform of Eq. (A3) will be evaluated. To this end, we will insert an intermediate sum over a complete basis of interacting electronic states:

$$\begin{aligned}[Y^{\mathrm{TO}}_{\mathbf{q},\mathbf{q}_1,\mathbf{q}_2}]_1(\omega,\omega_1,\omega_2)=&\int_{-\infty}^{+\infty}dtdt_1dt_2\frac{e^{i\omega t}e^{i\omega_1t_1}e^{i}\omega_2t_2}{2\langle\Psi_0|\Psi_0\rangle}\Theta(t-t_1)\Theta(t_1-t_2)\\&\times\sum_{l,m}\langle\Psi_0|n^I_{\mathbf{q}}(t)|\Psi_l\rangle\langle\Psi_l|n^I_{\mathbf{q}_1}(t_1)|\Psi_m\rangle\langle\Psi_m|n^I_{\mathbf{q}_2}(t_2)|\Psi_0\rangle.\end{aligned} \tag{A5}$$

If the following representation of the Heaviside function,

$$\Theta(t)=\frac{-1}{2\pi i}\int_{-\infty}^{+\infty}d\omega\frac{e^{i\omega t}}{\omega+i\eta}, \tag{A6}$$

is used in Eq. (A5), we find

$$[Y^{\mathrm{TO}}_{\mathbf{q},\mathbf{q}_1,\mathbf{q}_2}]_1(\omega,\omega_1,\omega_2) = -\frac{1}{2\langle\Psi_0|\Psi_0\rangle}\int_{-\infty}^{+\infty} dt dt_1 dt_2 e^{i\omega t} e^{i\omega_1 t_1} e^{i\omega_2 t_2} \times \int_{-\infty}^{+\infty}\frac{d\omega_a}{2\pi}\frac{e^{i\omega_a(t-t_1)}}{\omega_a+i\eta}\int_{-\infty}^{+\infty}\frac{d\omega_b}{2\pi}\frac{e^{i\omega_b(t_1-t_2)}}{\omega_b+i\eta}\sum_{l,m}\langle\Psi_0|n^I_{\mathbf{q}}(t)|\Psi_l\rangle\langle\Psi_l|n^I_{\mathbf{q}_1}(t_1)|\Psi_m\rangle\langle\Psi_m|n^I_{\mathbf{q}_2}(t_2)|\Psi_0\rangle. \tag{A7}$$

Once the integrations over the ω_a and ω_b internal variables are done in Eq. (A5), we obtain

$$[Y^{\mathrm{TO}}_{\mathbf{q},\mathbf{q}_1,\mathbf{q}_2}]_1(\omega,\omega_1,\omega_2) = \sum_{l,m}\frac{\pi\delta(\omega+\omega_1+\omega_2)\,\delta^3(\mathbf{q}+\mathbf{q}_1+\mathbf{q}_2)\,n^{0l}_{\mathbf{q}}n^{lm}_{\mathbf{q}_1}n^{m0}_{\mathbf{q}_2}}{(\omega-E_l-E_0+i\eta)(\omega_2-E_0-E_m-i\eta)}, \tag{A8}$$

where $n^{lm}_{\mathbf{q}}$ represents

$$n^{lm}_{\mathbf{q}} = \langle\Psi_l|n_{\mathbf{q}}|\Psi_m\rangle, \tag{A9}$$

and E_m indicates the energy of the state $|\Psi_m\rangle$. Both δ functions [$\delta(\omega+\omega_1+\omega_2)$ and $\delta^3(\mathbf{q}+\mathbf{q}_1+\mathbf{q}_2)$], which appear in Eq. (A9), are a consequence of the time and space invariance of the medium in equilibrium, respectively.

If we perform the same evaluation with each of the terms that appear in Eq. (A3) we reach to the definite spectral analysis of the time-ordered quadratic response function:

$$Y^{\mathrm{TO}}_{\mathbf{q},\mathbf{q}_1,\mathbf{q}_2}(\omega,\omega_1,\omega_2) = \pi\delta(\omega+\omega_1+\omega_2)\,\delta^3(\mathbf{q}+\mathbf{q}_1+\mathbf{q}_2)\sum_{l,m}\left\{\frac{n^{0l}_{\mathbf{q}}n^{lm}_{\mathbf{q}_1}n^{m0}_{\mathbf{q}_2}}{(\omega-E_l-E_0+i\eta)(\omega_2-E_0-E_m-i\eta)} + \frac{n^{0l}_{\mathbf{q}_1}n^{lm}_{\mathbf{q}}n^{m0}_{\mathbf{q}_2}}{(\omega_1-E_l-E_0+i\eta)(\omega_2-E_0-E_m-i\eta)} + \frac{n^{0l}_{\mathbf{q}_1}n^{lm}_{\mathbf{q}_2}n^{m0}_{\mathbf{q}}}{(\omega_1-E_l-E_0+i\eta)(\omega-E_0-E_m-i\eta)} + 1\Leftrightarrow 2\right\}. \tag{A10}$$

Now, we have to do the same with the retarded quadratic response function expanded in the following way:

$$Y^{R}_{\mathbf{q},\mathbf{q}_1,\mathbf{q}_2}(t,t_1,t_2) = \frac{1}{2}\left\{\Theta(t-t_1)\Theta(t_1-t_2)\frac{\langle\Psi_0|n^I_{\mathbf{q}}(t)n^I_{\mathbf{q}_1}(t_1)n^I_{\mathbf{q}_2}(t_2)|\Psi_0\rangle}{\langle\Psi_0|\Psi_0\rangle} - \Theta(t-t_1)\Theta(t_1-t_2)\frac{\langle\Psi_0|n^I_{\mathbf{q}_1}(t_1)n^I_{\mathbf{q}}(t)n^I_{\mathbf{q}_2}(t_2)|\Psi_0\rangle}{\langle\Psi_0|\Psi_0\rangle} - \Theta(t-t_1)\Theta(t_1-t_2)\frac{\langle\Psi_0|n^I_{\mathbf{q}_2}(t_2)n^I_{\mathbf{q}}(t)n^I_{\mathbf{q}_1}(t_1)|\Psi_0\rangle}{\langle\Psi_0|\Psi_0\rangle} + \Theta(t-t_1)\Theta(t_1-t_2)\frac{\langle\Psi_0|n^I_{\mathbf{q}_2}(t_2)n^I_{\mathbf{q}_1}(t_1)n^I_{\mathbf{q}}(t)|\Psi_0\rangle}{\langle\Psi_0|\Psi_0\rangle} + 1\Leftrightarrow 2\right\}. \tag{A11}$$

The second and seventh terms in Eq. (A11) may be reduced to only one when the following equality between Heaviside functions is used

$$\Theta(t-t_1)\Theta(t_1-t_2)+\Theta(t-t_2)\Theta(t_2-t_1) = \Theta(t-t_1)\Theta(t-t_2), \tag{A12}$$

and we have

$$[Y^R_2+Y^R_7]_{\mathbf{q},\mathbf{q}_1,\mathbf{q}_2}(t,t_1,t_2) = -\frac{1}{2}\Theta(t-t_1)\Theta(t_1-t_2)\frac{\langle\Psi_0|n^I_{\mathbf{q}_1}(t_1)n^I_{\mathbf{q}}(t)n^I_{\mathbf{q}_2}(t_2)|\Psi_0\rangle}{\langle\Psi_0|\Psi_0\rangle}. \tag{A13}$$

The same process can be applied with the third and sixth terms in Eq. (A11). After this simplification, the retarded expression contains six terms, the same as the time-ordered one we want to compare with.

We can develop the same procedure as the one followed with the time-ordered response function, in order to obtain the spectral analysis of the retarded quadratic response function. We find

$$Y^R_{\mathbf{q},\mathbf{q}_1,\mathbf{q}_2}(\omega,\omega_1,\omega_2)=\pi\delta(\omega+\omega_1+\omega_2)\,\delta^3(\mathbf{q}+\mathbf{q}_1+\mathbf{q}_2)\sum_{l,m}\left\{\frac{n^{0l}_{\mathbf{q}}n^{lm}_{\mathbf{q}_1}n^{m0}_{\mathbf{q}_2}}{(\omega-E_l-E_0+i\eta)(\omega_2-E_0-E_m-i\eta)}\right.$$
$$\left.+\frac{n^{0l}_{\mathbf{q}_1}n^{lm}_{\mathbf{q}}n^{m0}_{\mathbf{q}_2}}{(\omega_1-E_l-E_0-i\eta)(\omega_2-E_0-E_m-i\eta)}+\frac{n^{0l}_{\mathbf{q}_1}n^{lm}_{\mathbf{q}_2}n^{m0}_{\mathbf{q}}}{(\omega_1-E_l-E_0-i\eta)(\omega-E_0-E_m+i\eta)}+1\Leftrightarrow 2\right\}. \tag{A14}$$

The only difference between the time-ordered and the retarded quadratic response functions is the sign of the imaginary part of the frequency. We can deduce from Eq. (A14) that the frequency variables always appear in the retarded function in the following way: $\omega+i\eta$, $\omega_1-i\eta$, and $\omega_2-i\eta$. Therefore, it may be considered as an analytical function on these variables and can be directly obtained from a proper expression of the time-ordered response function. Due to the developed prescription, we orient our effort to obtain first an approximation for the time-ordered response function, where the reversible quantum field theory may be applied.

*Electronic address: wmbvejaa@lg.ehu.es

[1] J. Neufeld and R. H. Ritchie, Phys. Rev. **98**, 1632 (1955); **99**, 1125 (1955).

[2] V. N. Neelavathi, R. H. Ritchie, and W. Brandt, Phys. Rev. Lett. **33**, 302 (1974); **33**, 670(E) (1974); **34**, 560(E) (1975).

[3] M. H. Day, Phys. Rev. B **12**, 514 (1975); V. N. Neelavathi and R. H. Kehr, *ibid.* **14**, 4229 (1976); R. H. Ritchie, W. Brandt, and P. M. Echenique, *ibid.* **14**, 4808 (1976); M. H. Day and M. Ebel, Phys. Rev. B **19**, 3434 (1979).

[4] P. M. Echenique, R. H. Ritchie, and W. Brandt, Phys. Rev. **20**, 2567 (1979).

[5] A. Mazarro, P. M. Echenique, and R. H. Ritchie, Phys. Rev. B **27**, 4117 (1983).

[6] W. H. Barkas, W. Birnbaum, and F. M. Smith, Phys. Rev. **101**, 778 (1956); W. H. Barkas, N. J. Dyer, and H. H. Heckman, Phys. Rev. Lett. **11**, 26 (1963); **11**, 138(E) (1963).

[7] A. Faibis, R. Kaim, I. Plesser, and Z. Vager, Nucl. Instrum. Methods **170**, 99 (1980); A. Breskin, A. Faibis, G. Goldring, M. Hass, R. Kaim, Z. Vager, and N. Zwang, *ibid.* **170**, 93 (1980).

[8] H. Esbensen and P. Sigmund, Ann. Phys. (Leipzig) **201**, 152 (1990).

[9] A. Arnau and E. Zaremba, Nucl. Instrum. Methods Phys. Res. B **90**, 32 (1994).

[10] J. J. Dorado, O. H. Crawford, and F. Flores, Nucl. Instrum. Methods Phys. Res. B **93**, 175 (1994); **95**, 144 (1995).

[11] A. Bergara, J. M. Pitarke, and R. H. Ritchie, Nucl. Instrum. Methods Phys. Res. B **115**, 70 (1996).

[12] C. C. Sung and R. H. Ritchie, Phys. Rev. A **28**, 674 (1983).

[13] C. D. Hu and E. Zaremba, Phys. Rev. B **37**, 9268 (1988).

[14] J. M. Pitarke, R. H. Ritchie, P. M. Echenique, and E. Zaremba, Europhys. Lett. **24**, 613 (1993); J. M. Pitarke, R. H. Ritchie, and P. M. Echenique, Nucl. Instrum. Methods Phys. Res. B **79**, 209 (1993).

[15] J. M. Pitarke, R. H. Ritchie, and P. M. Echenique, Phys. Rev. B **52**, 13 883 (1995).

[16] J. M. Pitarke and R. H. Ritchie, Nucl. Instrum. Methods Phys. Res. B **90**, 385 (1994); I. Campillo and J. M. Pitarke, *ibid.* **115**, 75 (1996).

[17] A. Bergara and J. M. Pitarke, Nucl. Instrum. Methods Phys. Res. B **96**, 604 (1995).

[18] J. M. Pitarke, A. Bergara, and R. H. Ritchie, Nucl. Instrum. Methods Phys. Res. B **99**, 87 (1995).

[19] R. Cenni and P. Saracco, Nucl. Phys. A **487**, 279 (1988); R. Cenni, F. Conte, A. Cornacchia, and P. Saracco, Nuovo Cimento **15** (12), 1 (1992).

[20] C. F. Richardson and N. W. Ashcroft, Phys. Rev. B **50**, 8170 (1995).

[21] J. M. Rommel and G. Kalman, Phys. Rev. E **54**, 3518 (1996).

[22] W. Bernard and H. Callen, Rev. Mod. Phys. **31**, 1017 (1959).

[23] A. L. Fetter and J. D. Walecka, *Quantum Theory of Many Particle Systems* (McGraw-Hill, New York, 1971); A. A. Abrikosov, L. P. Gorkov, and I. E. Dzyaloshinkii, *Methods of Quantum Field Theory in Statistical Physics* (Prentice-Hall, Englewood Cliffs, NJ, 1962).

[24] See, e.g., D. Pines and P. Nozières, *The Theory of Quantum Liquids*, Vol. I (Addison Wesley, New York, 1989).

[25] P. M. Echenique, F. Flores, and R. H. Ritchie, in *Solid State Physics*, edited by E. H. Ehrenreich and D. Turnbull (Academic, New York, 1990), Vol. 43; P. M. Echenique, F. J. Garcia de Abajo, V. H. Ponce, and M. E. Uranga, Nucl. Instrum. Methods **96**, 583 (1995).

[26] L. V. Keldysh, Sov. Phys. JETP **20**, 1018 (1965).

[27] N. F. Mott and H. S. W. Massey, *The Theory of Atomic Collisions*, 3rd ed. (Oxford University Press, New York, 1987), p. 57.

[28] C. O. Almbladh, U. von Barth, Z. D. Popovic, and M. J. Stott, Phys. Rev. B **14**, 2250 (1976).

[29] C. Zhang, N. Tzoar, and P. M. Platzman, Phys. Rev. B **37**, 7326 (1988).